

## SCIENTIFIC NOTE

### POSSIBILITY OF GROUNDWATER OCCURRENCES IN THE UPPER 30 M OF THE DAMMAM FORMATION, USING ELECTRICAL SURVEY, WEST OF AL-SALMAN DEPRESSION, SOUTH IRAQ

#### INTRODUCTION

The groundwater is one of the most precious of all natural resources, particularly in arid and semi-arid lands. Generally, the Arabian Peninsula is one of these lands, where present-day rainfall is scarce and limited to mountainous areas. The rest of the land must depend on other sources of water, especially groundwater. The groundwater in the Southern Desert is relatively deep and brackish. For this purpose, a project report has been submitted to GEOSURV to explore new sources of high quality water in an area that lies at the western and southern parts of Al-Salman Depression in the Iraqi Southern Desert (Al-Bahadily, 2012).

The purpose of this scientific note is to explore the groundwater that may be present as fresh water in perched aquifers, which occur near the ground surface within the carbonate beds. It is achieved by electrical method through studying the lateral changes in resistivity.

The present study includes performance of two electrical measuring lines, located at a distance of about 5 Km from the southern and western rims of Al-Salman Depression. The studied area is defined by the coordinates 44° 15' to 44° 45' E and 30° 00' to 30° 45' N.

#### GEOLOGICAL SETTING

The studied area is a part of the Southern Desert, which generally has flat rocky terrain, associated with ridges and karst depressions (Hassan *et al.*, 1995). The exposed Dammam Formation (Eocene) is mainly composed of nummulitic limestone with marl, and about 200 m in thickness in the type locality. Quaternary sediments are represented by depression fill sediments (Fig.1). Anhydrite and gypsum beds of Russ Formation (subsurface) are totally dissolved. The covering layers sag into solution cavities forming a kind of Dolines, karst holes and valley sinks (Al-Mubarak and Amin, 1983). Structurally, the regional strike of the beds is NW – SE with dip amount estimated as (2 – 3)° towards the northeast. The main valleys have almost parallel and narrow courses; drain the area from the southwest to the northeast (Hassan *et al.*, 1995 and Jassim and Goff, 2006).

The Dammam and Umm Er Radhumma formations represent the main upper aquifers within the study area. The static water level ranges from (150 – 350) m, below the surface, and there are two directions of groundwater flow; one from west to east, the other from south to north and northwest. The quality of the groundwater is slightly brackish to brackish water (Al-Jiburi and Al-Basrawi, 2012).

#### ARCUATED FEATURES IN THE SATELLITE IMAGE

Remote sensing provides a cost-effective methodology for identifying potential groundwater sources. Generally, the geological features such as faults and drainage patterns (both active and ancient) may point to areas where groundwater is concentrated (El-Baz, 1995 and Burnett, 2011).

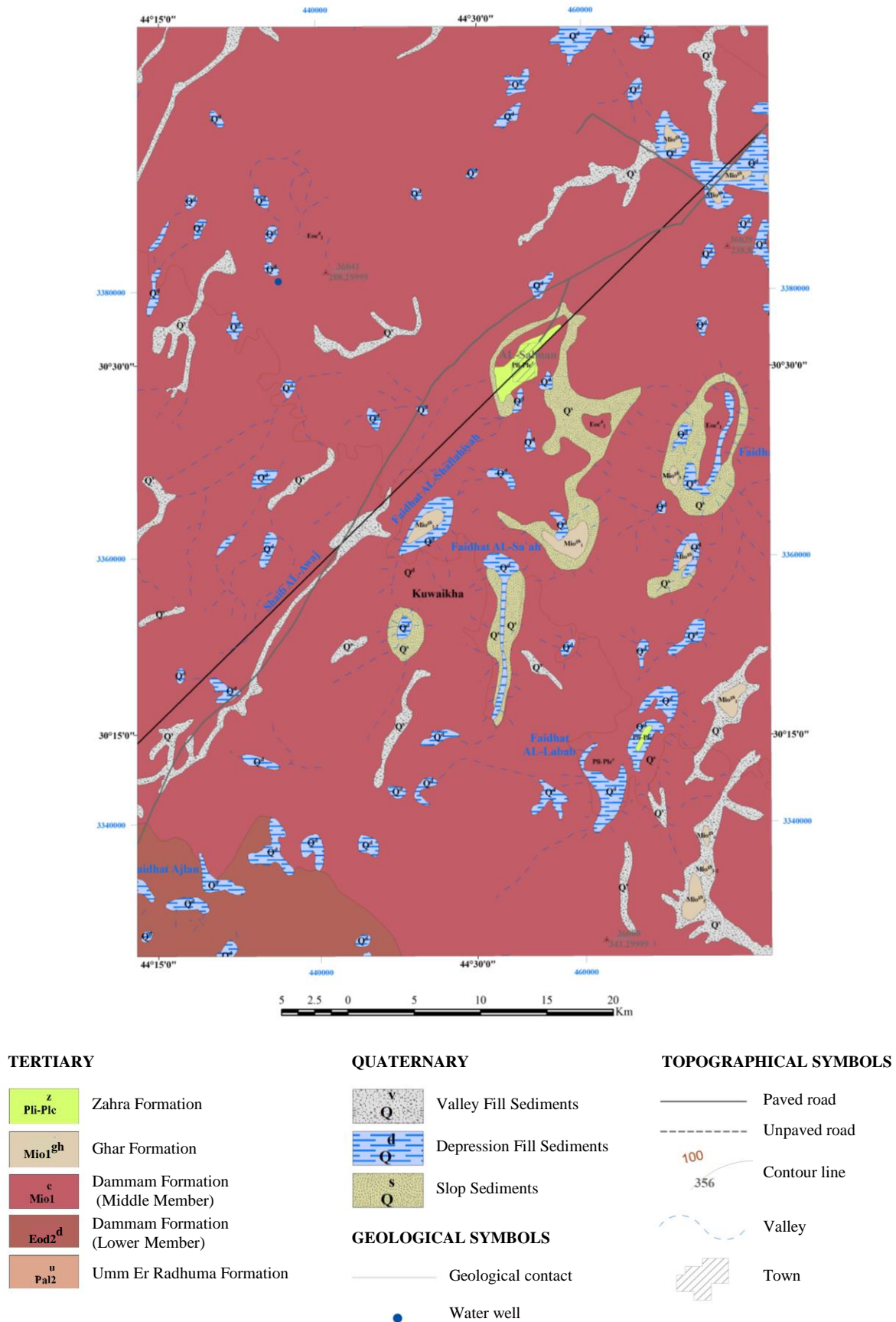


Fig.1: Geological map of the study area and surroundings (after Yacoub *et al.*, 2012)

Jassim and Goff (2006) reported that the satellite image of the study area (Fig.2) shows tracing of arcuate features that may be related to buried or abandoned river systems, which are features associated with present day valley courses. They need to be investigated in details due to their importance in groundwater exploration. Moreover, the image shows enormous circular forms that indicate different types of karst forms (Sissakian *et al.*, 2013).

Three preferable locations are selected for performing the electrical survey. The first is the arcuate features, and the second is depressions-fill sediments, and the third is a relatively small and nearly circular karst form, which is covered by Quaternary sediments.

## FIELD WORK

The field work included following-up the arcuate features and performing the two profiles. Wenner array, of electrode spacing (**a**) equals (5, 10, 15, 20, 25 and 30) m, is used. The measuring lines **A** and **B** in Fig. (2) pass across the geological features mentioned in the previous section; so that the optimum contrast in the apparent resistivity is obtained. According to the separation between the electrodes (**a**), the maximum penetration depth of the survey is about 30 m.

**Line A:** This line is located about 5 Km from the western rim of Al-Salman Depression. It is executed across relatively small depression fill sediments, and it has nearly NW – SE direction. The total length of this line is 200 m, and it includes 9 measuring points; from A1 to A9, with spacing interval of 25 m. The results of the apparent resistivity ( $\rho_a$ ) with the corresponding values of **a** are given in Table (1).

**Line B:** This line is located to the west of the southwestern rim of Al-Salman Depression at a distance of about 4.7 Km. It is executed across a relatively small circular karst form of about 650 m diameter and 7 m deep, which is covered by Quaternary sediments. The total length of this line is 590 m, and includes 11 measuring points; from B1 to B11, with a spacing interval of about 50 m. The results of the apparent resistivity ( $\rho_a$ ) with the corresponding values of **a** are given in Table (2).

## RESULTS

### ▪ Arcuate Features

Following-up the arcuate features by direct field observations at three separate locations (1, 2 and 3 in Fig.2), showed that these features are related to residual chert that cover relatively broad depression surrounded by rims (Fig.3). These rims are elevated few meters above the surrounding areas and are covered by either thin soil; mainly of sand, or rock fragments. However, locally, the limestone of Dammam Formation is exposed; therefore, performing electrical measurements on these rocks is impossible.

### ▪ Geoelectrical Pseudosections

The geoelectrical pseudosections for the two measuring lines; A and B are constructed as shown in Fig. (4a and b), respectively.

— **The Lateral Variations in Apparent Resistivity Along Measuring Line A:** Figure (4a) displays the lateral variations in " $\rho_a$ " across a small depression fill sediments, the resulting apparent resistivity values are grouped as four distinctive zones. These zones are about (400, 600, 800 and 1200)  $\Omega.m$ .



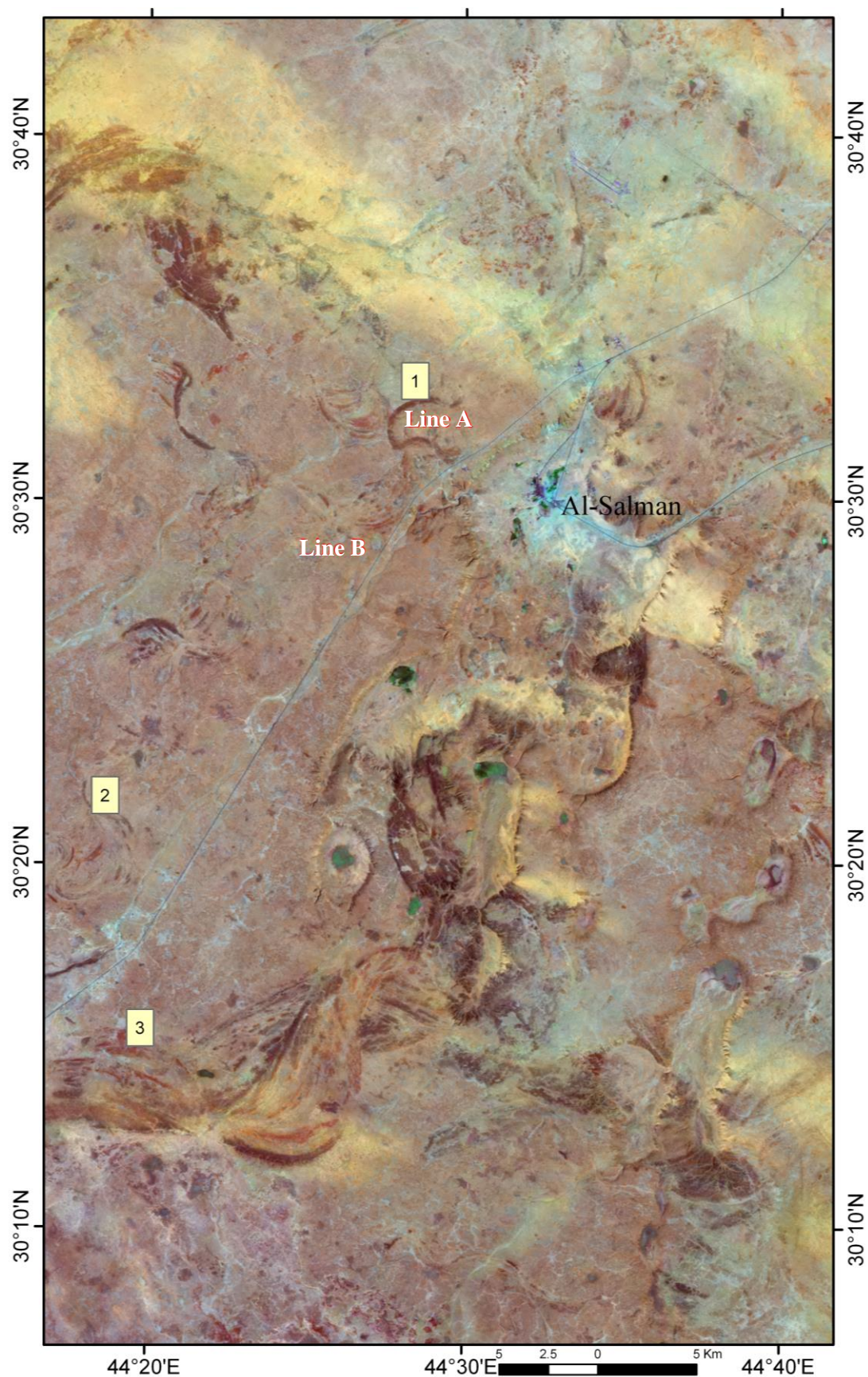


Fig.2: Satellite image of the study area shows the arcuated features

— **The Lateral Variations in Apparent Resistivity Along Measuring Line B:** Figure (4b) displays the apparent resistivity values across the circular karst form. The values are grouped as three distinctive zones; about (80, 150 and 450)  $\Omega.m$ . A fence diagram is plotted to explain these variations (Fig.4c).

Table 1: Values of "pa" against the separation distance (a), along line A

a (m)	A1	A2	A3	A4	A5	A6	A7	A8	A9
5	534	502	580	659	816	1005	1193	440	440
10	188	345	550	754	1068	1583	1319	440	880
15	170	330	670	1008	1319	1875	1130	754	791
20	214	352	730	1017	1256	1796	1167	1005	628
25	251	361	640	926	1382	1382	1177	1099	549
30	94	396	550	772	1187	1112	942	848	470

Table 2: Values of "pa" against the separation distance (a), along line B

a (m)	B1	B2	B3	B4	B5	B6	B7	B8	B9	B10	B11
5	110	502	188	722	110	94	75	82	85	63	283
10	107	471	251	57	138	151	119	94	82	83	440
15	132	414	339	66	151	188	160	113	75	283	565
20	151	377	352	75	163	201	176	125	125	176	628
25	173	424	377	68	173	220	188	188	141	251	628
30	170	471	377	94	188	226	188	170	188	38	565



Fig.3: Chert covers the gentle rim

## **DISCUSSION AND CONCLUSIONS**

Field observation of the arcuate features observed in the satellite image of the study area (Fig.2) shows that these features are related to chert fragments that cover gentle rims, which apparently have the same tone as that of wet areas.

However, some of these features have different reflection coefficients; as for example the arcs that appear immediately to the NW of feature 1 and feature 2 in Fig. (2). These differences are attributed to the size and density of distribution of the fragments. Large size and relatively high density of chert fragments appear as a dark area (low reflection coefficient) and vice versa.

Obviously, the distribution of the apparent resistivity ( $\rho_a$ ) of lines A and B (Fig.4a and b) displays a complex picture. The range of " $\rho_a$ " is (57 – 1875)  $\Omega.m$ . Normally, the electrical boundaries separating layers of different resistivities, are controlled more by porosity, water content and water quality than by the resistivity of the rock matrix. These boundaries may or may not coincide with boundaries separating layers of different geological age or different lithological composition. Clay minerals, however, are capable of conducting electricity electronically, and the flow of current in a clay layer is both electronic and electrolytic (Zohdy *et al.*, 1980). Accordingly, this picture may be interpreted in terms of the weathering extent of the carbonate beds and the clay content, and in both of them small quantities of water (purchased water) may exist. The high values of the  $\rho_a$  ( $\geq 1200 \Omega.m$ ) may be interpreted as due to the limestone beds that are less affected by the weathering, while the low values of  $\rho_a$  ( $\leq 80 \Omega.m$ ) may be interpreted as due to the Quaternary clay sediments that cover the Dammam Formation and may also fill the cavities and the fractures of the limestone beds (weathered limestone). However, the values of " $\rho_a$ " that lie between (1200 – 80)  $\Omega.m$  may be interpreted to be the limestone beds that are weathered in different rates.

Moreover, this picture does not indicate the presence of the groundwater within the penetrated depth 30 m. Groundwater aquifers usually have very low values of apparent resistivity; it may be less than 2  $\Omega.m$ , due to high conductivity, especially, of the brackish water. However, the electrical measurements over the small depression; (**line A**) are higher than that over the circular karst (**line B**). This is related to the karst being an intake area of low land, 7 m deep, collecting the flowing water that come from nearby areas. Therefore, the water clearly decreases the values of " $\rho_a$ ". In addition, the collected water also increases the dissolution then collapsing the carbonate rocks to accelerate the evolution of the karst phenomena.

The survey shows that the subsurface topography of the Dammam Formation (not weathered beds) is totally different from the surface topography (weathered beds). High values of " $\rho_a$ " refer to high resistance or less affected by collapsing and dissolving of the limestone beds. However, finding out perched aquifers in such area (karst dominated) is a very hard work. On the other hand, the performance of gravity measurements over such areas should give numerous positive and negative anomalies in the local field, as confirmed by Al-Shaikh and Al-Mashhadani (2013).



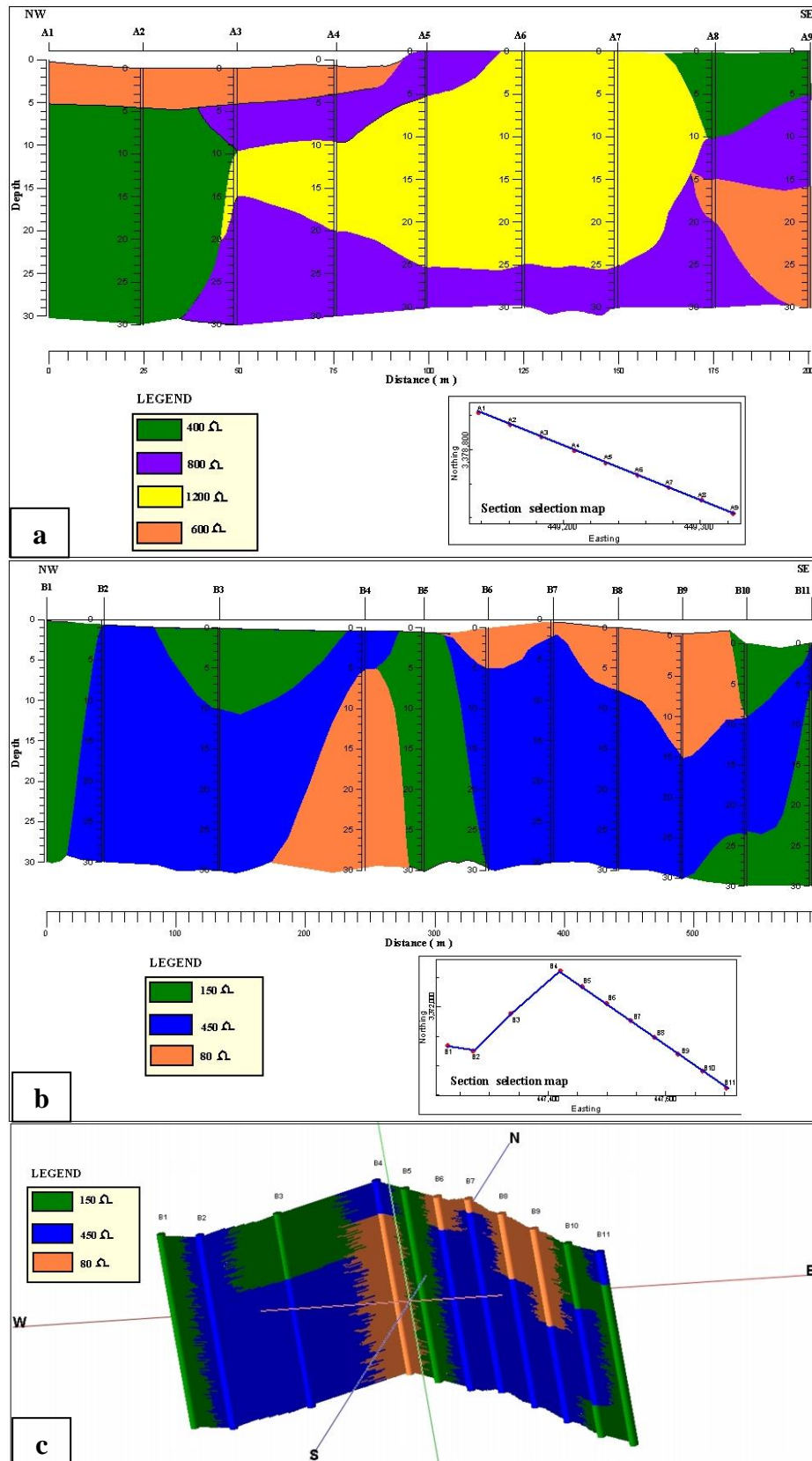


Fig.4: Geoelectrical pseudosections show: **a)** the lateral variations in "pa" across depression fill sediments, **b)** across circular karst form, and **c)** represents the fence diagram of karst measurements

**Hayder A. Al-Bahadily**, Assistance Chief Geophysicist, Iraq Geological Survey (GEOSURV), P.O. Box 986, Baghdad, Iraq.

**e-mail:** [hayder.adnan@geosurviraq.com](mailto:hayder.adnan@geosurviraq.com)

**Sabah O. Abdul Qadir**, Senior Chief Geophysicist, Iraq Geological Survey (GEOSURV), P.O. Box 986, Baghdad, Iraq.

**e-mail:** [sabahkirkuk@yahoo.com](mailto:sabahkirkuk@yahoo.com)

**Khansa'a T. Hussein**, Assistance Chief Engineer, Iraq Geological Survey (GEOSURV), P.O. Box 986, Baghdad, Iraq.

## **REFERENCES**

- Al-Bahadily, H.A., 2012. Detailed electrical survey for groundwater exploration on arcuated features, west of Al-Salman Depression. Project report. GEOSURV, archive of Geophysics Division.
- Al-Jiburi, H.K. and Al-Basrawi, N.H., 2012. Hydrological and hydrochemical study of Al-Salman Quadrangle (NH-38-6), scale 1:250 000. GEOSURV, int. rep. no. 3381.
- Al-Mubarak, M.A. and Amin, R.M., 1983. Report on the regional geological mapping of the eastern part of the Western Desert and the western part of the Southern Desert. GEOSURV, int. rep. no. 1380.
- Al-Shaikh, Z.D. and Al-Mashhadani, A.M., 2013. A gravity study of the Nukhaib Depression area, Western Desert of Iraq. Iraqi Bull. Geol. Min., Vol.9, No.1, p. 35 – 49.
- Burnett, D.O., 2011. Use of Remote Sensing for Groundwater Mapping in Haiti in Articles. Water Availability, University of Montevallo, 7pp.
- El-Baz, F., 1995. Utilizing satellite images for ground water exploration in fracture zone aquifers. In: Water resources management in arid countries. Muscat, Sultanate of Oman, 436pp.
- Hassan, K.M., Yacoub, S.Y. and Amir, E.A., 1995. The Geology of Al-Salman Quadrangle (NH-38-6), scale 1: 250 000. GEOSURV, int. rep. no. 2404.
- Jassim, S.Z. and Goff, J.C., 2006. Geology of Iraq. Dolin, Prague and Moravian Museum, Brno, 341pp.
- Yacoub, S.Y., Hassan, K.M., Mahdi, A.I. and Hassan, E.A., 2012. Geological map of Al-Salman Quadrangle (NH-38-6), scale 1: 250 000. GEOSURV, Baghdad, Iraq.
- Sissakian, V.K., Mahmoud, A.A. and Awad, A.M., 2013. Genesis and age determination of Al-Salman Depression, South Iraq. Iraqi Bull. Geol. Min., Vol.9, No.1, p. 1 – 16.
- Zohdy, A.A.R., Eaton, G.P. and Maybey, D.R., 1980. Application of Surface Geophysics to Groundwater Investigations. United States Government Printing Office, Washington, 116pp.